RSC Advances

ROYAL SOCIETY OF CHEMISTRY

www.rsc.org/advances

Motor coordination dysfunction induced by gold nanorods core /silver shell nanostructures in mice: disruption in mitochondrial transport and neurotransmitter release involved

Nan Yang[a,1], Yanyong Liu[a,1], Yinglu Ji[c], Zhili Ren[a], Jie Meng[b], Chao Ji[a], Jian Liu[b], Ji Zheng[a], Xiaochun Wu[c*], Pingping Zuo[a*] and Haiyan Xu[b*]

[a] Department of Pharmacology, Institute of Basic Medical Sciences, Chinese Academy of Medical Sciences & Peking Union Medical College, Beijing 100005, P. R. China. E-mail: pingping_zuo@126.com; Fax/Tel:+86-10-69156404.

[b] Department of Biomedical Engineering, Institute of Basic Medical Sciences, Chinese Academy of Medical Sciences & Peking Union Medical College, Beijing, 100005, P. R. China. E-mail: xuhy@pumc.edu.cn; Fax/Tel: +86-10-69156437.

[c] CAS Key Laboratory of Standardization and Measurement for Nanotechnology, National Center for Nanoscience and Technology, Beijing 100190, P. R. China.

E-mail: wuxc@nanoctr.cn; Tel: +86-10-82545577; Fax: +86-10-82545577.

[1] These authors contributed equally to this work.

Risk of silver nanoparticles (AgNPs) exposure is becoming increasingly widespread and causes great concern. Since AgNPs induce blood-brain barrier destruction and accumulate in the brain, it is of great significance to inquire its biological effects on central nervous system (CNS). This study selected gold core/silver shell nanostructures (for simplicity termed as silver nanorods, AgNRs) as a model for AgNPs and investigated the neurotoxicity and mechanism in mice by single dose of intracerebroventricular (i.c.v.) administration. Behavioral changes of the mice were weekly monitored by multiple behavioral tests. Significant reduction in residence time on Rota-rod treadmills was observed for AgNRs treated mice at all the test time-points after the administration, clearly indicating a motor coordination dysfunction. Pathological examination revealed significant loss of tyrosine hydroxylase (TH)-positive neurons in the substantia nigra pars compacta (SNpc) and TH-positive fibers in the striatum, which are two important brain regions regulating motor function. In primary mesencephalic neuron, both speed and percentage of mitochondrion moving in anterograde direction were decreased by AgNRs treatment, along with great reduction in neurotransmitter vesicle release efficacy. Taken together, *i.c.v* administrated AgNRs impaired the nigro-striatal pathway and disrupted the mitochondrial axonal transport and neurotransmitter release may underlie the motor coordination dysfunction.

Introduction

Silver nanoparticles (AgNPs) are increasingly applied in various fields, especially in medical healthcare, food package, fabrics and household appliance. For instance, AgNPs have been used as broad spectrum antimicrobial agents, [1] biosensors, [2] wound care products, [3,4]and even in washing machines, ink and clothing. [5,6] Despite there are rapidly increasing literatures reporting cytotoxicity of AgNPs, [7-11] their effects on animals' brain and behavior are rarely investigated. Some investigations evidenced that AgNPs could enter through blood-brain barrier (BBB) and accumulated in different regions of brain. For instance, Takenaka et al reported that there were significant amounts of silver in the blood, liver, kidney, spleen, heart and brain after rats were inhaled ultrafine elemental AgNPs. [12] When orally administrated with AgNPs (60 nm) over a period of 28 days, tissue samples were measured by an atomic absorption spectrophotometer and found accumulated in the Sprague-Dawley (SD) rat brain. [13] A few of possible pathways for AgNPs entering into brain were proposed, including passive diffusion, carrier-mediated endocytosis[14] and directly into brain by trans-synaptic transport. [15] It is now known that the biological half-life of silver in CNS is longer than in other organs. By prolonged administration of different silver compounds like silver lactate, silver nitrate and some silver proteins like Protargol, silver accumulated in neurons and glia. [16-18] These results suggest that silver could have significant physiological actions or pathological consequences to the brain, thus bring us much doubt on whether AgNPs cause neurotoxicity in human and animals and open much space for systemic investigation on neurotoxicity upon AgNPs exposure.

The aim of this work is to reveal AgNPs-induced neurotoxicity and behavioral changes in mice. We chose gold nanorods core/ silver shell nanostructures as a model for AgNPs (**Fig. 1**). The reasons of choosing such nanostructures include following: First, the unique rod-like shape made them easily distinguished in the tissue when performing ultrastructure observation. Second, the internal gold core endows the nanostructure superior optical response, such as a strong longitudinal surface plasmon resonance (SPR) band in near-infrared region. [24] Because only the silver shell was interfacing to the cells or tissues in the present exposure experiments, for simplicity, those core/shell nanostructures were termed as silver nanorods (AgNRs). Moreover, our recent studies showed that after subcutaneous injection of AgNRs, silver and gold contents in the subcutis and organs were examined by inductively coupled plasma mass spectrometry at different time points within 28 days. [34] We found that silver concentration in mice brain gradually increased, which was dissolved from the AgNRs. The obtained data spurred us to investigate the potential neurotoxicity and underlying mechanisms of AgNRs.

Experimental

Animals

Eighty adult male C57/BL6J mice were supplied by Weitonglihua Experimental Animal Centre (Beijing, China). Animals were randomly housed in polypropylene cages and maintained in a constant temperature (22 ± 1°C) and humidity (60 ± 10%) environment on a 12 h light-dark cycle (lights on at 7:00 AM). The animals had free access to food and water throughout the experiments. Animal treatment and maintenance were carried out in accordance the guidelines established by the National Institutes of Health for the care and

use of laboratory animals and were approved by the Animal Care Committee of the Peking Union Medical College and Chinese Academy of Medical Science.

Preparation of AgNRs stock solution

AgNRs was prepared according to the procedure described below. In preparation, 100 mL purified AuNRs was added to 50 mL 0.1 M CTAB aqueous solution containing AA (550 μL, 0.1 M), $AgNO_3$ (2 mL, 0.01 M) and NaOH (1.4 mL, 0.2 M). The solution was then shaken vigorously and put in a 30 °C water bath for 14 h. The AgNRs were centrifuged at 9000 rpm for 7 min to remove excess CTAB and other ions, and the precipitation was redispersed in 100 mL water. 5 mL of 20 mg/mL PSS (including 60 mM NaCl) was added. After mixing for 3 h, the solution was centrifuged at 9500 rpm for 10 min. The precipitation was redispersed in the desired volume of water and AgNRs coated by PSS were obtained. The Ag/Au mole ratio in AgNRs is 0.85 from ICP-AES measurement.

Chemicals and other materials

Rabbit anti-TH antibody and rabbit anti-NeuN antibody were products of Millipore. Polink-2 plus polymer HRP detection system for primary antibody was purchased from Beijing Zhongshan Biotechnology Co., China. B27 and Neurobasal medium were purchased from invitrogen. B-27 (Invitrogen).

I.c.v. administration of AgNRs

AgNRs solution for injection was prepared in double distilled water at the concentration of 14 nM. After being housed for 1 week prior to experiment, animals were randomly divided into 4 groups, corresponding to four AgNRs exposure duration of 1, 2, 3 and 4

weeks respectively. Every group was further divided into two subgroups (control and AgNRs treatment group). Mice were anesthetized by an intraperitoneal injection of 1% pentobarbital sodium and then fixed in the mouse brain stereotactic apparatus. After that, 2 μl of AgNRs solution or double distilled water as vehicle were stereotaxically injected at 1 mm lateral, 0.5 mm caudal to bregma, and 3 mm deep from the dura using a 5 μl Hamilton syringe. The injection rate was 1 μl/min and the syringe was kept in place for 1 min after injection to prevent backflow. After surgery, behavioral tests were performed at the scheduled time-points.

Open-field test

Open field behavior was measured using an automated device to assess spontaneous movement. [35] The apparatus consists of a rectangular box (50 × 50 × 40 cm) with a floor divided into 16 rectangular units. When performing the test, mice were placed individually into the center of the field and locomotor activity was quantified during a 5 minute observation period. The overall distance traveled and the number of square crossings was calculated by the system. The open-field was washed with a 75% ethanol solution before behavioral testing to eliminate possible bias due to odors left by previous rats.

Elevated Plus Maze

The elevated plus maze is a widely used test for assessing anxiety behavior in mice. [36,37] The apparatus was made of wood and consisted of two open arms (50 × 10 × 1 cm) and two closed arms (50 × 10 × 30 cm). Each open arm is divided in three equal sections for the observation of the open arms exploration. The open and closed arms intercross perpendicularly in a region corresponding to the central region (10 × 10 cm) of the

apparatus. The apparatus was elevated to a height of 65 cm above the floor level.

At least 1 h before testing, the mice were placed onto the central platform facing an enclosed arm. A 5-min trial was performed and, between subjects, the maze was thoroughly cleaned. Direct registrations were made by an observer sitting close to the maze using the following conventional parameters: number of open and closed arm entries (arm entry defined as all four paws entering an arm) and time spent on open arms (excluding the central platform). The observation was performed between 14:00-17:00.

Y maze test

Y-maze has three arms of equal size (60×11.5×25 cm). The animals were randomly placed in a "start" arm and the number of visits and the time spent in this arm, the novel (previously closed) arm, and the "other" arm were assessed by video tracking for a 8 min exploration phase.

Forced swimming test

The forced swim test was performed 24 h later after open field test.[35] The mouse was placed in a glass cylinder (20 cm in diameter, 24 cm high) filled with water at 23 ±1 °C to the height of 15 cm for 5 min. The time spent immobile (passive floating, when the animal was motionless or doing only slight movements with tail or one hind limb, whereas the animal was judged to be active when struggling, climbing or swimming using all four paws) was measured during the test.

Rotarod test

The ability of motor/coordination was assessed by Rota Rod. [25] Parameters were set as follow: initial speed 5 rpm; maximum speed 20 rpm; the time of acceleration was 300 s.

The duration of mice staying on the rotarod was recorded using stopwatch.

Tissue processing

After behavioral tests, animals were decapitated. Brains were immediately taken out and washed in ice-cold isotonic saline solution. Hippocampus and striatum tissues were isolated and kept frozen in liquid nitrogen before analysis.

In addition, other animals in each group were anesthetized via pentobarbital sodium and perfused transaortically first with 0.1 M PBS followed by 4% paraformaldehyde (pH 7.4). The brains were removed and postfixed in the same 4% paraformaldehyde solution at 4°C, after which they were equilibrated in 0.1 M PBS containing 15%, 20% and 30% sucrose at 4°C one by one. Coronal sections (35 μm) were cut using a cryostat.

Immunohistochemistry

Free-floating brain slices (35 μm thick) were washed in PBS to remove cryopreservative. The tissue was incubated for 30 min at room temperature in 3% H_2O_2 solution to reduce endogenous peroxidase activity, and then additionally washed in PBS. The samples were placed in bovine serum for 30min at room temperature. Incubation overnight at 4°C was performed with rabbit anti-TH-antibody (1:800) (Millipore) or mouse anti-NeuN-antibody (1:50) (Millipore). After incubation, the slices were washed with PBS and incubated with polymer Helper (Polink-2 plus polymer HRP detection system for rabbit primary antibody, Beijing Zhongshan Biotechnology Co., China) for 15min at room temperature, again washed, and then incubated in poly-HRP anti rabbit IgG / anti mouse IgG (Polink-2 plus polymer HRP detection system for primary antibody, Beijing Zhongshan Biotechnology Co., China) for 15min at room temperature. To develop color, the slices were incubated

briefly in DAB substrate kit. After a final set of washes in PBS, the slices were mounted on slides, dehydrated, cleared, and coverslipped with mounting medium.

Primary mesencephalic neuron culture

Mesencephalic neuron culture was performed according to methods described previously.[38,39] Briefly, tissue was dissected and enzymatically dissociated using HBSS supplemented with 10 mM HEPES and 0.25% trypsin for 30 min at 37 °C. Then it was stopped using DMEM medium containing serum. Finally the cells were plated at a density of 20,000 cells per well in poly-D-lysine and laminin coated 96-well plates for cell viability, 35 mm dishes for mitochondrial transport and glass Lab-Tek for vesicle release. The medium was exchanged toserum-free Neurobasal medium with 2% B27 supplement, 0.5 mM glutamine, 100 U penicillin and 100 U streptomycin per ml, followed by re-incubation for 7-8 days with half of the medium being changed every 3 days.

Cell culture and transfection

Neurons were transfected using X-tremeGENE HP DNA transfection reagent (Roche, Germany). For mitochondrial transport, we typically transfected the neurons on DIV6-7 and performed imaging on DIV8-9. Mito-EGFP was generously provided by Prof. Jianxin Kang at NIH/NIMH.

Live cell imaging of mitochondrial movement

Fluorescent time-lapse recordings were performed on the Live Cell Station (Olympus, Japan) using the Volocity imaging software.[40] For imaging of mitochondrial transport, we typically recorded neurons at a sampling rate of one frame every 5 s for 5 min, with the CCD exposure at 50 ms exposure and 2 × 2 binning. For each experiment, a population of

neurons was imaged for a 5 min time-lapse recording at 30 min after Ag application. Quantification of moving mitochondria was conducted by simply counting the number of moving mitochondria in each 5 min time-lapse sequence. A moving mitochondrion was defined as one that moved more than a distance of twice its length over the 5 min period.

FM 1-43 experiments

Neurons cultures were loaded with FM1-43 (10 μM; Invitrogen) in 45 mM of KCl depolarizing buffer (100 mM NaCl, 45 mM KCl, 2 mM $CaCl_2$, 2 mM $MgCl_2$, 5.5 mM glucose, 20 mM HEPES, pH = 7.3) for 2 min. Coverslips were then washed with low K^+ buffer (140 mM NaCl, 5 mM KCl, 2 mM $CaCl_2$, 2 mM $MgCl_2$, 5.5 mM glucose, 20 mM HEPES, pH 7.3) for 5 min to remove excess dye. Images were acquired with a Cascade II EMCCD camera on an Olympus X61 inverted microscope. Images were collected with 200 ms exposures at 1 s intervals during dye destaining. A baseline was collected for 10 images before addition of depolarizing buffer to destain the boutons. Dye-labeled bouttons were selected as regions of interest in Image-Pro Plus 5.0 (Media Cybernetics) and fluorescence intensity was plotted versus time. Destaining traces were normalized by setting maximal load to 1 and complete destaining (disappearance of bouton to background levels) to zero for comparison of rates.

Statistical analysis

The density of positive cells in histochemistry analysis was calculated by Image-Pro Plus 5.0 image analysis software. Experimental data were analyzed statistically using one-way analysis of variance followed by post-hoc test. Summarized data were expressed as mean ± SEM. Statistical significance was set at $p < 0.05$. All Statistical analysis was undertaken

using SPSS v11.5.

Results and Discussion

Fig. 1A is extinction spectra of the AgNRs and their corresponding gold nanorod cores. The AgNRs are prepared by gold nanorod-templated growth. The inner gold nanorod exhibits a strong LSPR band at 830 nm. After deposition of 1 nm thick Ag shell, the LSPR band blue-shifts to 690 nm with increased intensity. Due to different LSPR positions, their suspensions show different colors (reddish brown for the gold NRs and green for Ag NRs). Considering the toxicity of CTAB, we used PSS to coat CTAB layer to avoid the toxic effect of CTAB. The effect of PSS coating AgNRs have been demonstrated in our early studies.[34] Therefore, the AgNRs are coated with two layers: a CTAB bilayer and then an electrostatic adsorbed negatively charged PSS layer, as schematically shown in **Fig. 1B**. The PSS layer is more biocompatible than CTAB layer. The morphology of the AgNRs is characterized by AFM **(Fig. 1C)**. They have a mean thickness ca. 10 nm (by height image). In phase image, the deep color in rod edges suggests the soft materials on the surface of the AgNRs.

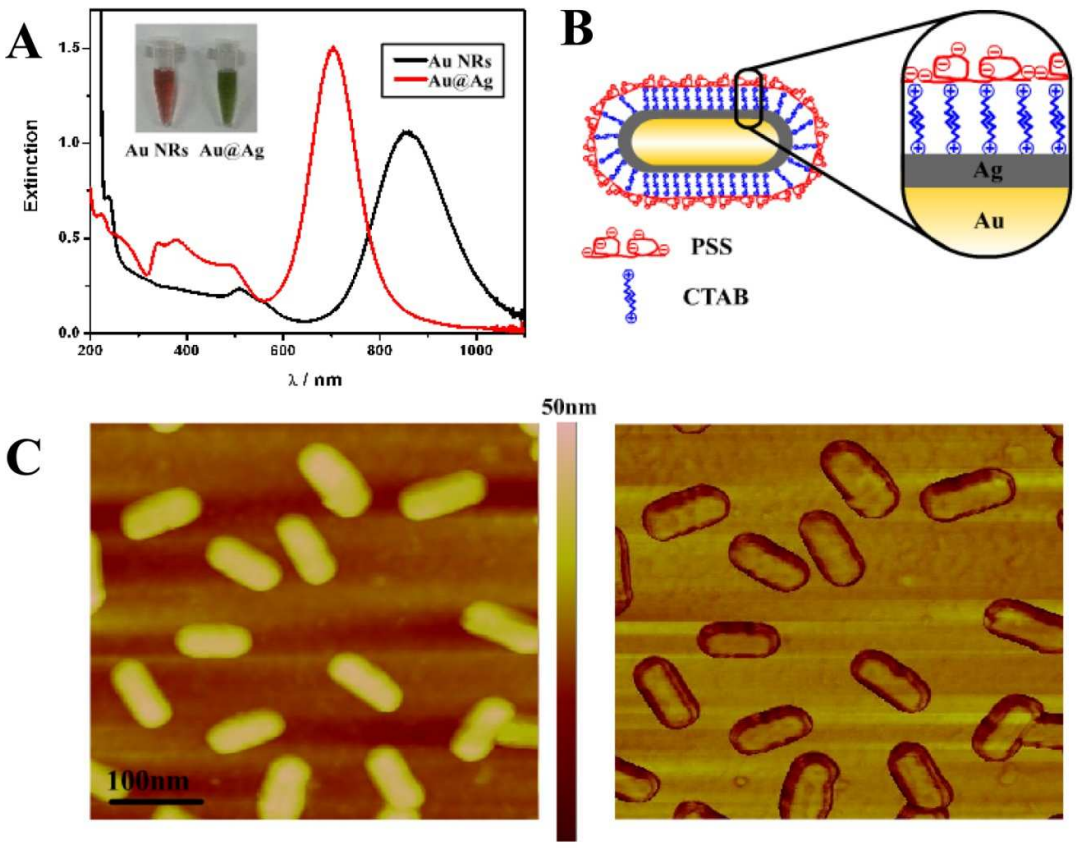

Fig. 1 (A)Extinction spectra of the AgNRs and their corresponding gold NRs core dispersed in water. (B) Schematic of the AgNRs used for mice experiments. (C) AFM images of the AgNRs with height and phase mode.

After given single dose of AgNRs by intracerebroventricular (i.c.v.) administration, the mice behaviors were assessed using multiple behavioral measurements associated with potential neurological disorder, including Rota-rod test, Y-maze test, forced swim test, elevated plus maze and open field test. Except for the results of Rota-rod test, we did not observe any obvious changes in cognition and mental function after the AgNRs administration. The Rota-rod test is a reliable index for evaluating motor coordination of mouse. [25] By performing this test, we found that the residence time on Rota-rod treadmills

was shorter in AgNRs treated mice at all the designated time-points, when compared with that of control mice (**Fig. 2**). Further comparison showed that the residence time was reduced up to 70% for all the four groups, indicating that motor coordination of the mice was significantly injured within 4 weeks after AgNRs injection.

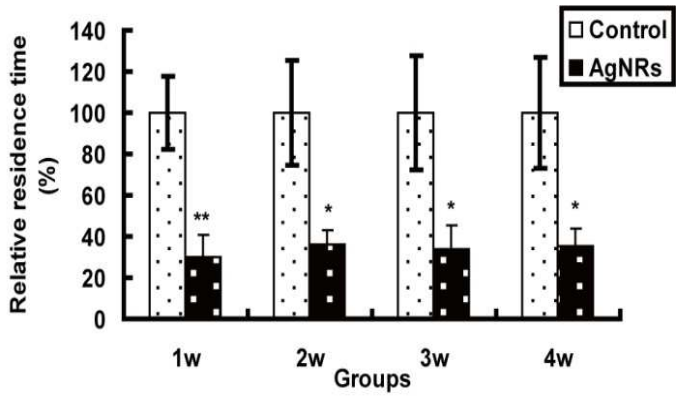

Fig. 2 Effects of intracerebroventricularly administrated AgNRs on mice motor function. Relative residence time of the mice on Rota-rod treadmills was affected significantly by AgNRs within 4 weeks post single dose of intracerebroventricular administration. Data were shown as mean ± SEM, n=8-10 in each group. *$p<0.05$, **$p<0.01$ vs. control group.

Motor behavior is regulated by the midbrain dopaminergic nigro-striatal system which consists of two brain structures: compact zone of substantia nigra (SNpc) and striatum. Main kind of cells located in SNpc is dopaminergic (DA-ergic) neuron and their axons are projected along the nigrostriatal tract to the striatum. Tyrosine hydroxylase (TH) is the specific marker of DA-ergic neuron. The abnormal motor behavior implied DA-ergic neuron was affected. In order to figure out whether and how i.c.v. administrated AgNRs caused the behavioral change, we first investigated the effects of AgNRs on the fate of Tyrosine hydroxylase (TH) -positive neurons in SNpc and the concomitant loss of TH fiber in striatum by immunohistochemistry method. **Fig. 3A** presented a representative

photograph of TH-stained sections of the SNpc. TH-positive neurons were seen in dark brown (circled by rectangle). Significant loss of TH-positive neurons in the SNc was observed in all the AgNRs groups in reference to the corresponding control groups, evidenced by reduction of the dark brown color. Stereological counting provided a quantitative result, showed a dramatically reduction of TH-positive neurons at 1 week post injection, followed by slight recovery increase at 2, 3, and 4 week (**Fig. 3B**). Corresponding to the density variation of TH-positive neurons, TH-positive fibers in the striatum were similarly significantly decreased (**Fig. 4**). Except for that at the 2 week, the reduction percentage of TH-positive fibers for the 1,3and 4 week was similar. Therefore, the substantial DA neuron damage in the SNpc and degradation of DA-ergic axons in the striatum constituted the material base for the movement disorders. It is noticeable that the injected AgNRs mostly aggregated in the area around the injection site and the edge zone of striatum. There were rare AgNRs observed in the compact zone of substantia nigra (SNpc) and inside of striatum. It has been demonstrated by several groups that silver nanoparticles released Ag^+ from their surface [27-30] and gave Ag^+ pressure to the bacteria. [31-32] Our previous study also demonstrated that AgNRs disrupting the cell membrane, because dissolved Ag^+ oxidized the cell membrane which allowed calcium influx and eventually led to the cells apoptosis. [33] The influence of lysosome in Ag^+ dissolution from sliver nanoparticle was recently well investigated, indicating that ligand bond stability plays an important role in determination of Ag species evolution.[42] Hence it is reasonably presumed that the significant reduction of TH-positive neurons and TH-positive fibers was mainly attributed to the Ag^+ dissolved from the surface of the injected AgNRs.

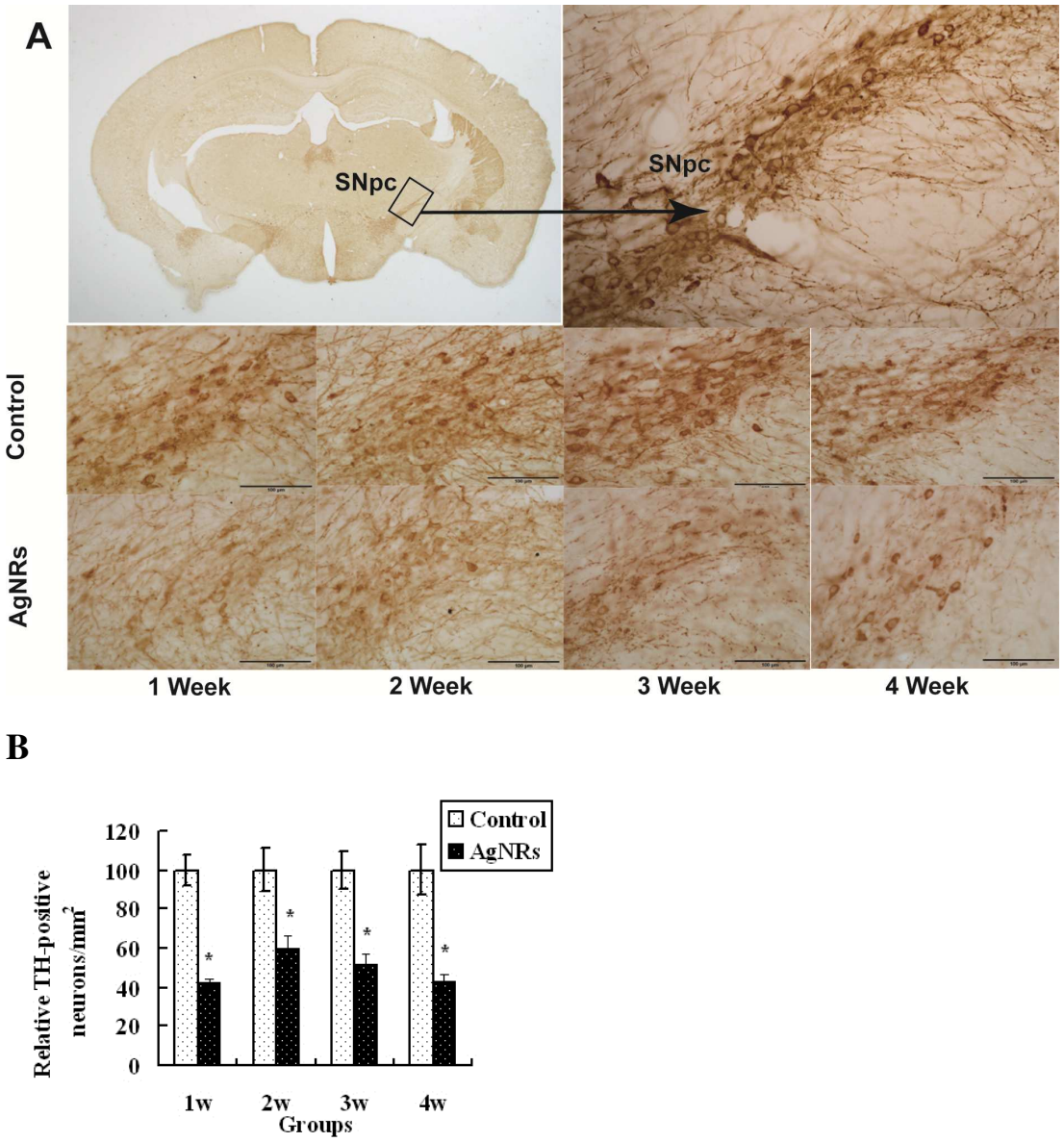

Fig. 3 Effects of AgNRs treatment on TH-positive neurons density in SNpc. (**A**) Representative photograph of TH-stained sections of SNpc . (**B**) Statistical analysis of TH-immunoreactive cell counts from the SNpc. Data are given as mean ± SEM, n=4-5 for each group, *p<0.05, **p<0.01 vs. control group.

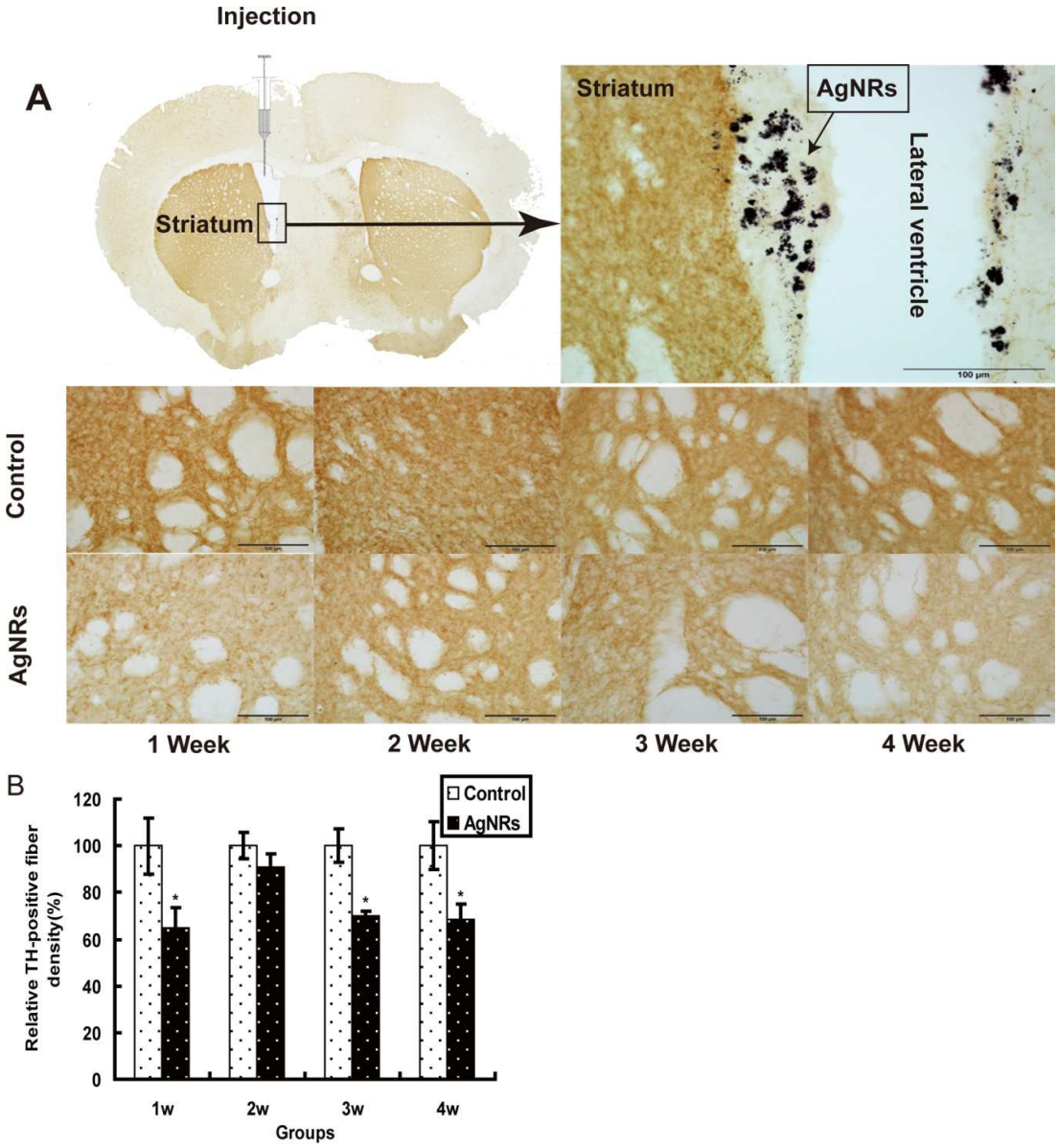

Fig. 4 Effects of AgNRs treatment on TH-positive fiber density in the striatum. (**A**) Representative image of striatum indicating that administrated AgNRs penetrated the ependyma into the striatum. (**B**) Statistical analysis of the TH-positive fiber density in the striatum. Data was represented as mean ± SEM, n=4-5 in each group. *p<0.05 vs. control group.

The behavioral and neuropathological changes induced by AgNRs treatment drew our attention to the neurodegenerative disease-Parkison's disease (PD), because PD is

characterized mainly by motor coordination dysfunction with neuropathological feature of degeneration of the nigrostriatal dopaminergic system. Existing evidences indicated that impaired axonal transport played an important role in PD process. [19] Postmortem studies on PD patients show widespread axonal pathology that appears to precede the loss of cell bodies. [20] Hence next we investigated the effects of AgNRs on the axonal transport in primary cultured mesencephalic neuron. Under fluorescent microscope, mitochondrial movement was seen in axons and representative moving mitochondrion was in the rectangle area (**Fig. 5A**). When the AgNRs were added in the culture medium for 4, 24 and 48 h, the percentage of anterograde moving mitochondria in the axons was significantly decreased (**Fig. 5B**), meanwhile the percentage of stationary mitochondria was increased (**Fig. 5C**). Moreover, AgNRs treatment did not affect mitochondrial moving speeds in the anterograde direction but increased that moving in the retrograde direction (**Fig. 5D**). Mitochondria with high membrane potential (used as a proxy for mitochondrial health) seemed to preferentially migrate in the anterograde direction, whereas mitochondria with low membrane potential (used as a proxy for mitochondrial damage) seemed to move in the retrograde direction. [21] Hereby, healthy mitochondria were specifically transported to distal regions with high-energy requirements, and impaired mitochondria were specifically returned to the cell soma for repair or destruction. Our results indicated AgNRs actually damage the neuronal mitochondria. The block of mitochondrial trafficking will result in mitochondrial redistribution away from the synapse back to the soma. Conceivably, damaged mitochondria moving toward the soma could deliver signals from the axon to the cell body, leading to the initiation of cell death.

Recently, Tay et al demonstrate that nanoparticles such as TiO_2 or SiO_2 disrupted the intracellular microtubule assembly. [41] Since mitochondrial transport along the neuronal axon is carried along microtubules, it is possible that AgNRs induced effect on the microtubules to interfere the trafficking. Because mitochondria are a vital energy-producing cell organelle to maintain the normal function, disturbed distribution of mitochondria away from sites of high ATP usage would lead to axonal impairment, loss of synaptic connectivity and function.

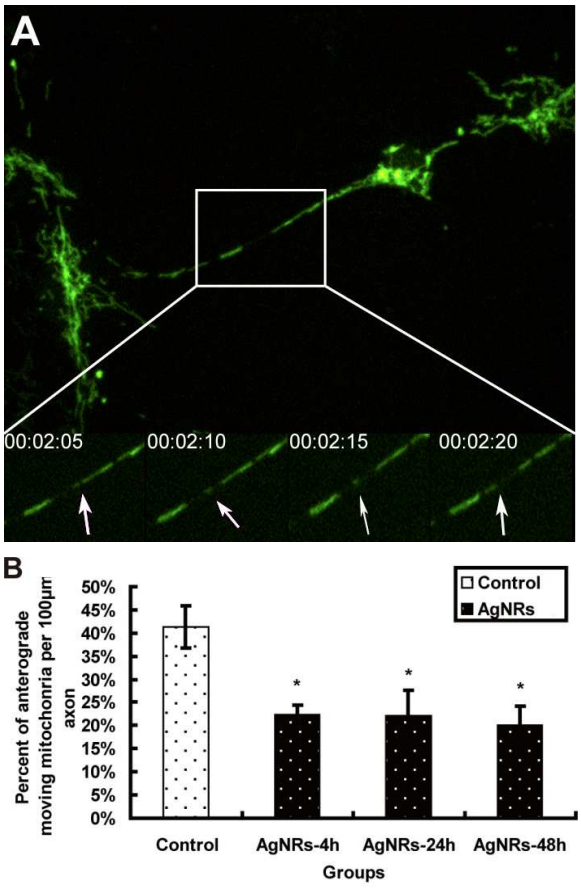

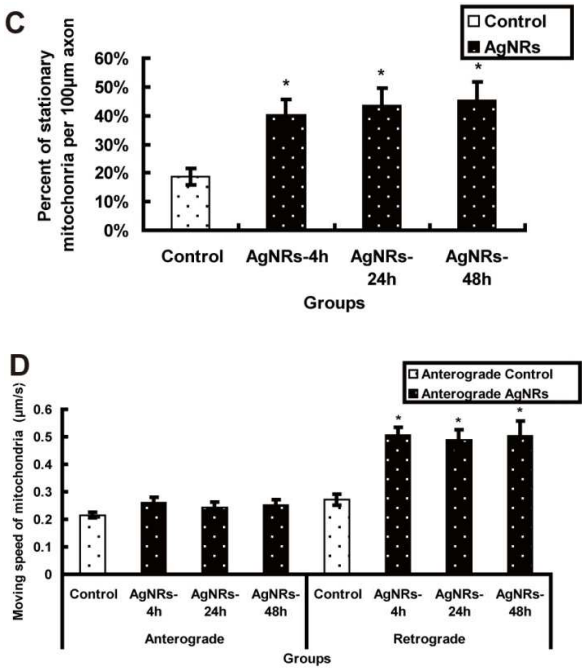

Fig. 5 AgNRs rapidly decreases mitochondrial movement in axons. (**A**) Representative view frame of mitochondrial movement along the axon, mitochondria move along the axon shown in a rectangle area; The arrow pointed to the track of an anterograde moving mitochondrion. Percent of anterograde moving (**B**) and stationary mitochondria（**C**）per 100 μm length of axon was calculated. Meanwhile, the speed of moving mitochondria was also analyzed (**D**). Bars represent the mean ± SEM of 3 independent experiments conducted in duplicate. *p< 0.05 vs. control group.

In neurons, the synaptic terminals are sites of high energy demand requiring mitochondria to produce high levels of energy for neurotransmitter vesicle release.[22] To investigate the secondary effect of AgNRs induced mitochondrial damage, FM1-43 was employed to directly measure the efficacy of synaptic neurotransmitter release in the cultured mesencephalic neurons. FM® styryl dyes, which have a high membrane affinity, allow direct monitoring of vesicle release and uptake in presynaptic terminals in

dissociated neuronal cultures, yielding valuable insights into transmitter release.[26] The release efficacy was obtained by calculating the percentage of remaining FM1-43 fluorescent intensity after high K^+ stimulus in the total FM1-43 loading intensity. Our results showed that 2 h short time exposure to AgNRs potentiated the neurotransmitter release; however 24 h and 48 h exposure significantly decreased the efficacy of neurotransmission release compared with the control neuron. It is clearly seen that more and more synaptic vesicles (stained in red fluorescence) were blocked with AgNRs extended exposure time (**Fig. 6**).

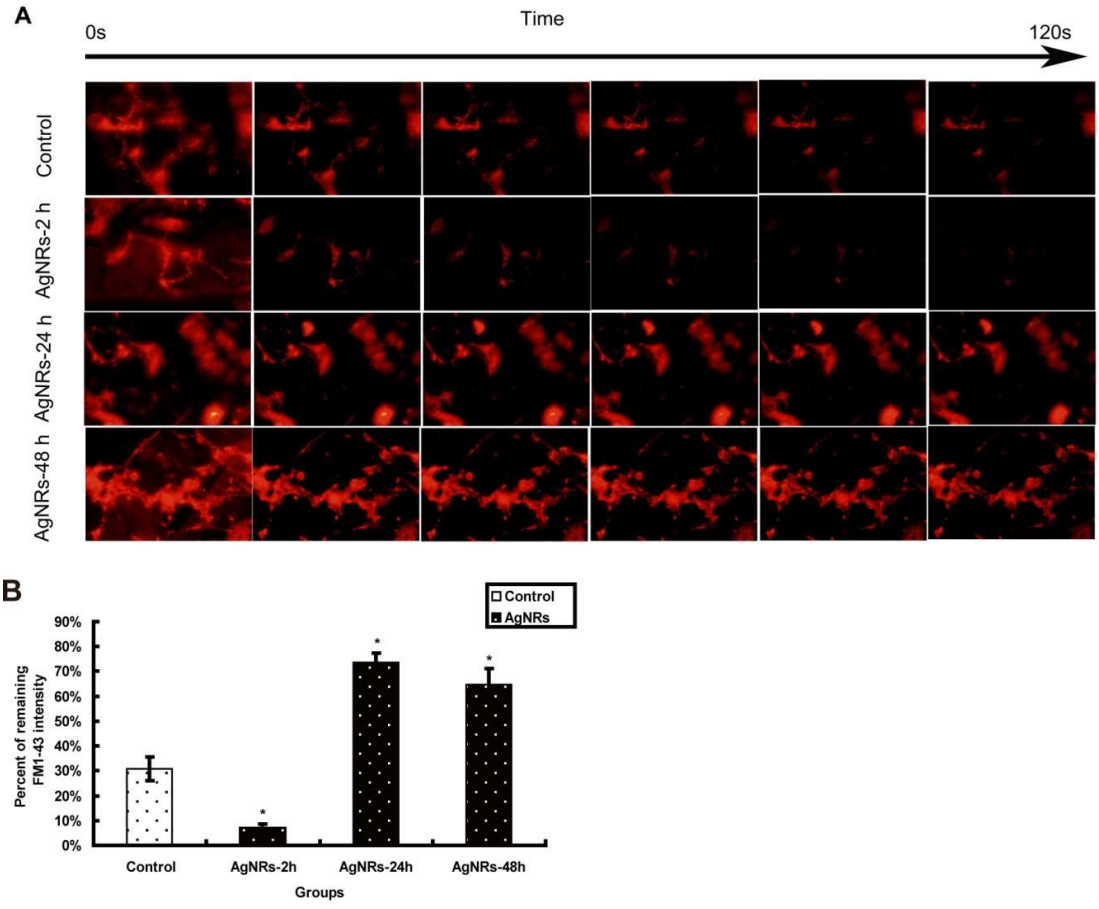

Fig. 6 Analysis of synaptic vesicle release efficacy using FM1-43 in primary cultured mesencephalic neurons. **(A)** The representative time-relapse destaining of synaptic

boutons of AgNRs groups for control, 2 h, 24 h, and 48 h. **(B**) Analytical results of synaptic vesicle release efficacy. Bars represent the mean ± SEM of 3 independent experiments conducted in duplicate. *$p < 0.05$ vs. control group.

Conclusion

Taken together, it is schematically summarized (**Fig. 7**) that *i.c.v* administrated AgNRs inhibited the mitochondrial axonal transport and neurotransmission, which eventually lead to the motor coordination dysfunction. To our best knowledge, the present work firstly revealed impact of AgNRs exposure to the neural system and animal motion behavior in the mouse model of i.c.v. administration. The experimental results provided useful information for potential risk evaluation when silver NPs penetrating blood-brain-barrier and entering into the brain. It should be pointed that as toxicological mechanisms of silver nanoparticles to the central nervous system are very complicated and involved many aspects, [44] further investigations are needed to perform to reveal the underlying pathological foundation.

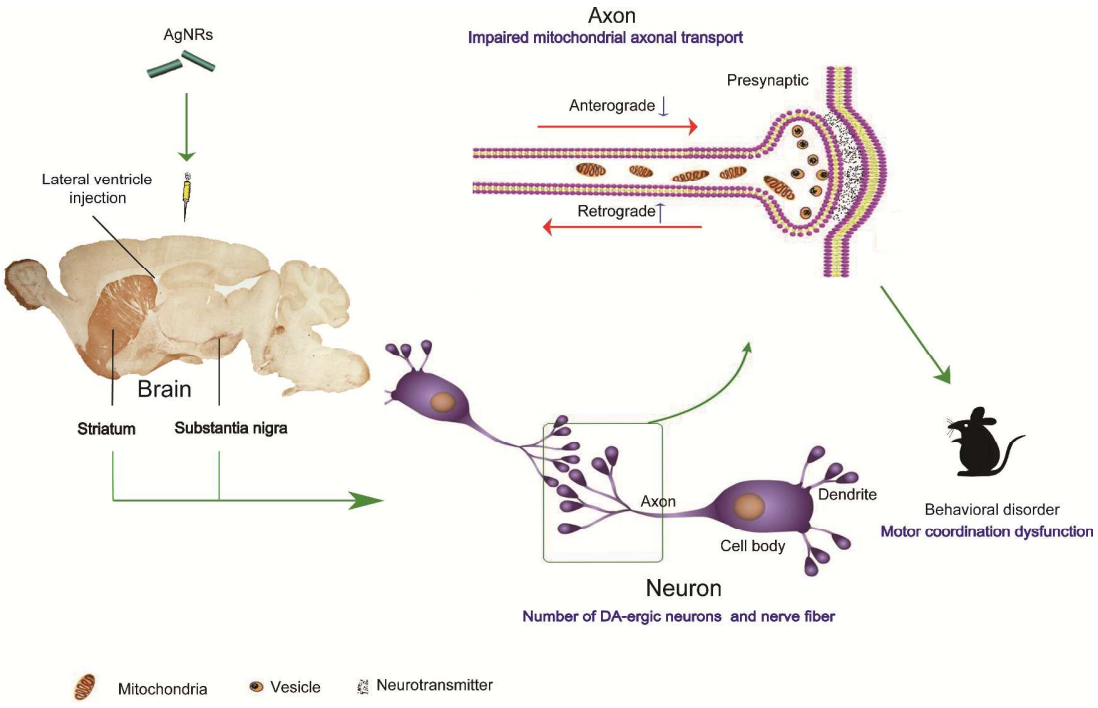

Fig. 7 Schematic graph showed that *i.c.v* administrated AgNRs affected nerve fiber density and neuron viability in the striatum and SNpc respectively, mainly due to the inhibition of mitochondrial axonal transport, which eventually leads to the motor coordination dysfunction.

ACKNOWLEDGMENTS

This work was supported by National Key Program of China (973 program 2010CB934002, 2011CB933504 and 2011CB932802).

Notes and references

1 K.J. Kim, W.S. Sung, B.K. Suh, S.K. Moon, J.S. Choi, J.G. Kim, D.G. Lee. *Biometals*, 2009, **22**, 235-242.

2 H. Sun, T.S. Choy, D.R .Zhu, W.C. Yam, Y.S. Fung. *Biosens. Bioelectron,*2009, **24**, 1405-1410.

3 S. Lu, W. Gao, H.Y. Gu. *Burns*, 2008, **34**, 623-628.

4 P. Muangman, C. Chuntrasakul, S. Silthram, S. Suvanchote, R. Benjathanung, S.Kittidacha, S.Rueksomtawin. *J. Med. Assoc. Thai.,* 2006, **89**, 953-958.

5 H.Y. Lee, H.K. Park, Y.M.Lee, K. Kim, S.B. Park. *Chem. Commun. (Camb.)*, 2007, **28**, 2959-2961.

6 N. Vigneshwaran,; A.A. Kathe, P.V. Varadarajan, R.P. Nachane, R.H. Balasubramanya. *J. Nanosci. Nanotechnol.*, 2007, **7**, 1893-1897.

7 S.M. Hussain, K.L.Hess, J.M.Gearhart, K.T.Geiss, J.J.Schlager. *Toxicol. In Vitro*, 2005, **19**, 975-983.

8 A. Burd, C.H. Kwok, S.C. Hung, H.S. Chan, H. Gu, W.K. Lam, L. Huang. *Wound Repair Regen.,* 2007, **15**, 94-104.

9 L. Braydich-Stolle, S. Hussain, J.J. Schlager, H. Marie-Claude, M. *Toxicol. Sci.*, 2005, **88**, 412-419.

10 W.J. Trickler, S.M. Lantz, R.C. Murdock, A.M. Schrand, B.L. Robinson, G.D. Newport, J.J. Schlager, S.J. Oldenburg, M.G. Paule, W.Jr. Slikker, S.M. Hussain, S.F. Ali. *Toxicol. Sci.*, 2010, **1**, 160-170.

11 M. Ahamed, M.S. Alsalhi, M.K. Siddiqui. *Clin. Chim. Acta*, 2010, **411**,1841-1848.

12 S. Takenaka, E. Karg, C. Roth, H. Schulz, A. Ziesenis, U. Heinzmann, P. Schramel, J. Heyder. *Environ. Health Perspect.*, 2001, **4**, 547-551.

13 Y.S. Kim, J.S. Kim, H.S. Cho, D.S. Rha, J.M. Kim, J.D. Park, B.S. Choi, R. Lim, H.K. Chang, Y.H. Chung, I.H. Kwon, J. Jeong, B.S. Han, I.J. Yu. *Inhal. Toxicol.,* 2008, **20**, 575-583.

14 P.H. Hoet, I. Bruske-Hohlfeld, O.V. Salata. *J. Nanobiotechnol.*, 2004, **2**, 12.

15 G. Oberdorster, Z. Sharp, V. Atudorei,; A. Elder, R. Gelein, W. Kreyling, C. Cox. *Inhal. Toxicol.,* 2004, **16**,437-445.

16 K.G. Scott, J.G. Hamilton. *Publ. Pharmacol.*,1950, **2**, 241-262.

17 J.E. Furchner, C.R. Richmond, G.A. Drake. *Health Phys.*,1968, **15**, 505-514.

18 J. Rungby, G.Danscher. *Acta Neuropathol.,* 1983, **60**, 92-98.

19 K.J.De Vos, A.J.Grierson, S.Ackerley, C.C. Miller. *Annu. Rev. Neurosci.*, 2008, **31**, 151-173.

20 S.Orimo, T.Uchihara, A.Nakamura, F.Mori, T.Ikeuchi, O.Onodera, M.Nishizawa, A.Ishikawa, A.Kakita, K.Wakabayashi, H.Takahashi. *Acta Neuropathol.*,2008, **116**, 575-577.

21 K.E.Miller, M.P.Sheetz. *J. Cell. Sci.*,2004, **117**, 2791-2804.

22 J.P. Bolanos, A. Almeida. *IUBMB Life,* 2010, **62**, 14-18.

23 C.V.Ly, P.Verstreken. *Neuroscientist*,2006, **12**, 291-299.

24 H.Sauer, W.H. Oertel. *Neuroscience,*1994, **59**, 401–415.

25 J.Liu, H.Wang, L. Zhang, Y. Xu, W. Deng, H.Zhu, C.Qin. *Arch. Med. Res.,*2011, 42, 1-7.

26 M.A.Gaffield, W.J Betz. *Nat. Protoc.,*2006, **1**, 2916-2921.

27 He W.; Zhou, Y.T.; Wamer W.G.; Boudreau M.D.; Yin, J.J. *Biomaterials*, 2012, **33**, 7547-7555.

28 C.Damm, H. Münstedt. *Appl. Phys. A*, 2008, **91**, 479-486.

29 J.M.Zook, S.E.Long, D.Cleveland, C.L.Geronimo, R.I.MacCuspie. *Anal. Bioanal.*

*Chem.,*2011, **401**, 1993-2002.

30 S.Kittler, C.Greulich, J.Diendorf, M. Koller, M. Epple. *Chem. Mater*,2010, **22**, 45-48.

31 M.M. Babu, J.Sridhar, P.Gunasekaran. *J. Nanobiotechnology*, 2011, **9**, 49.

32 J.S.McQuillan, H. Groenaga Infante, E.Stokes, A.M.Shaw. *Nanotoxicology*, 2012, **6**, 857-866.

33 X.Cheng, W. Zhang, Y. Ji, J. Meng, H. Guo, J. Liu, X. Wu, H. Xu. *RSC Adv.,* 2013, **3**, 2296-2305.

34 J.Meng, Y. Ji, J. Liu, X. Cheng, H. Guo, W. Zhang, X. Wu, H. Xu. *Nanotoxicology*, 2014, **8**, 686-696.

35 Y. Liu, N.Yang, W. Hao, Q. Zhao, T. Ying, S. Liu, Q. Li, Y. Liang, T. Wang, Y. Dong, C. Ji, P. Zuo. *Neurochem. Int.*, 2011,**58**, 904-913.

36 M.C. Norte, R.M. Cosentino, C.A. Lazarini. *Phytomedicine*, 2005,**12**,294-298.

37 L.H. Jacobson, B. Bettler, K. Kaupmann, J.F. Cryan. *Psychopharmacology (Berl)*, 2007, **190**, 541-53.

38 H.M. Gao, B. Liu, J.S. Hong. *J. Neurosci.*, 2003,**23**, 6181-6187.

39 J. Peng, X.O. Mao, F.F. Stevenson, M. Hsu, J.K. Andersen. *J. Biol. Chem.*, 2004, **279**,32626-32632.

40 J.S. Kim-Han, J.A. Antenor-Dorsey, K.L. O'Malley. *J. Neurosci.*, 2011, **31**,7212-7221.

41 C. Y. Tay, P. Cai, M. I. Setyawati, W. Fang, L. P. Tan, C. H. L. Hong, X. Chen, D. T. Leong. Nano Lett., 2014,**14**, 83-88.

42 M.I. Setyawati, X. Yuan, J. Xie, D.T. Leong. *Biomaterials*, 2014,**35**, 6707-6715.

43 C. Y. Tay, M.I. Setyawati, J. Xie, W. J. Parak, D.T. Leong. *Adv. Funct. Mater.,* 2014,

DOI: 10.1002/adfm.201401664.

44 Q. Mu, G. Jiang , L. Chen, H. Zhou , D. Fourches, A.Tropsha , B. Yan. *Chem. Rev.,* 2014, **114**,7740-7781.